

Spectroscopic Determination of Very Low Quantum Yield of Singlet Oxygen Formation Photosensitized by Dyes and Pigments

Shoichi Yamaguchi^a, Kimiya Takeshita^b,

Yutaka Sasaki^a, Yukichi Murata^b, and Tetsuo Murayama^b

^aCenter for Analytical Chemistry and Science, Inc.

1000 Kamoshida-cho, Aoba-ku, Yokohama 227-0033, Japan

^bMitsubishi Chemical Corporation

1000 Kamoshida-cho, Aoba-ku, Yokohama 227-8502, Japan

Abstract

We have measured the quantum yield Q_{Δ} of $^1\Delta_g$ molecular oxygen (singlet oxygen, 1O_2) formation photosensitized by some dyes for industrial uses, because the photofading processes of dyes are usually triggered by 1O_2 . Q_{Δ} for industrial dyes, however, is generally very low, and it has been difficult to determine accurately Q_{Δ} for them. We have made a highly sensitive spectrometer for 1.27- μm 1O_2 phosphorescence detection, and determined Q_{Δ} for an azo dye as low as $(2.2 \pm 1.5) \times 10^{-5}$. This is the first demonstration of Q_{Δ} lower than 10^{-4} as far as we know. Relationship between Q_{Δ} and the lightfastness of practical dyes is also discussed in this study.

Introduction

Molecular oxygen in the excited $^1\Delta_g$ state (1O_2) is a highly reactive species, and has been regarded as one of the most important reaction intermediates in photobiology and photochemistry. 1O_2 is characterized by near-infrared (NIR) phosphorescence at 1.27 μm . Technological improvements in the detection of the 1O_2 NIR emission are very important from biochemical and medical viewpoints, because 1O_2 phosphorescence emitted from living systems is very weak.¹ An excellent technique of weak-phosphorescence detection is expected also in the field of industrial chem-

istry, because it is widely believed that 1O_2 plays an essential role in oxidative photofading processes of some industrial dyes and pigments for practical uses.²⁻⁶ Even though 1O_2 photosensitized by industrial dyes causes the photofading of themselves, Q_{Δ} of these dyes is much lower than that of highly efficient photosensitizers such as porphyrin and terthiophene derivatives, whose Q_{Δ} ranges from 0.5 to 0.8.^{7,8} Actually all the Q_{Δ} values for industrial practical dyes reported to date lie in the range of 10^{-3} to 10^{-4} .^{3,6,7,9} The measurements of Q_{Δ} less than 10^{-3} have been realized only by the photochemical substrate-consumption method.

There have been few works which apply spectroscopic methods of 1.27- μm phosphorescence detection to the determination of low Q_{Δ} . Stracke et al.¹⁰ showed for the first time that it is possible to measure a 1O_2 phosphorescence spectrum photosensitized by rhodamine 6G (R6G), which is known as the most efficient laser dye and usually not regarded as a 1O_2 photosensitizer. We are going to show in this paper that Q_{Δ} for R6G is 8.3×10^{-3} . The intensity of the 1O_2 phosphorescence is proportional to the 1O_2 phosphorescence quantum yield Q_p as well as Q_{Δ} . Q_p in air-saturated acetonitrile is about 3×10^{-5} ,¹¹⁻¹⁵ and therefore the product $Q_{\Delta}Q_p$, which indicates the phosphorescence intensity, is 2×10^{-7} in Stracke's R6G measurement. Schmidt and Tanielian have recently demonstrated that quantitative time-resolved measurements of the 1O_2 phosphorescence are possible under conditions of very strong quenching.¹⁶ They ob-

tained a $^1\text{O}_2$ phosphorescence decay curve with a good signal to noise ratio under the condition of $Q_\Delta Q_p = 3 \times 10^{-7}$. Beeby and co-workers have reported a novel electronic switch which eliminates obstructive fluorescence contributions from a $^1\text{O}_2$ phosphorescence decay curve.¹⁷

There are two purposes in our present study: one is to establish a spectroscopic method of very low Q_Δ determination, and the other is to elucidate a determinant factor of dye lightfastness. We report the measurements of $^1\text{O}_2$ phosphorescence spectra photosensitized by industrial dyes for practical uses. We have made a highly sensitive spectrometer which is capable of even Raman spectroscopy. The spectrometer has enabled us to determine Q_Δ as low as 2.2×10^{-5} and $Q_\Delta Q_p$ as 7×10^{-10} . This is the first demonstration of Q_Δ lower than 10^{-4} . We present Q_Δ for xanthene, styryl, and azo dyes depicted in Chart 1. It is noted that the styryl dye (dye **I**) is the most fundamental molecule among commercially-used red dyes for thermal-transfer printing, and the azo dye (dye **II**) is one of arylazonaphthols which are most frequently used azo dyes. We have known that dyes **I** and **II** are both inferior in lightfastness for practical purposes. We discuss relationship between Q_Δ and the lightfastness of the dyes from the viewpoint of excited-state kinetics.

Experimental Section

Chart 1 shows the structural formulae of all the compounds used in the present study. RB (= rose bengal, Aldrich), R6G (= rhodamine 6G, Exciton, laser grade), dye **II** (= solvent red 1, Orient Chemical), DABCO (= 1,4-diazabicyclo[2.2.2]octane, Aldrich), and acetonitrile (Kanto Chemical, fluorometry grade) were used as received. Dye **I** was synthesized in our laboratory. The concentrations of all the photosensitizers (RB, R6G, dyes **I** and **II**) in acetonitrile were so controlled that the absorbance at 532 nm was set to 1.95 cm^{-1} . The sample solutions were kept in an open standard quartz cuvette of $1 \text{ cm} \times 1 \text{ cm} \times 4.5 \text{ cm}$. A beam from a diode-pumped continuous-wave Nd:YVO₄ laser (Spectra Physics, Millennia Vi) illuminated the sample solution across the base of the cuvette. The wavelength of the excitation laser beam was 532 nm, and the average power was 0.20 W. The photoexcited area of the solution along the

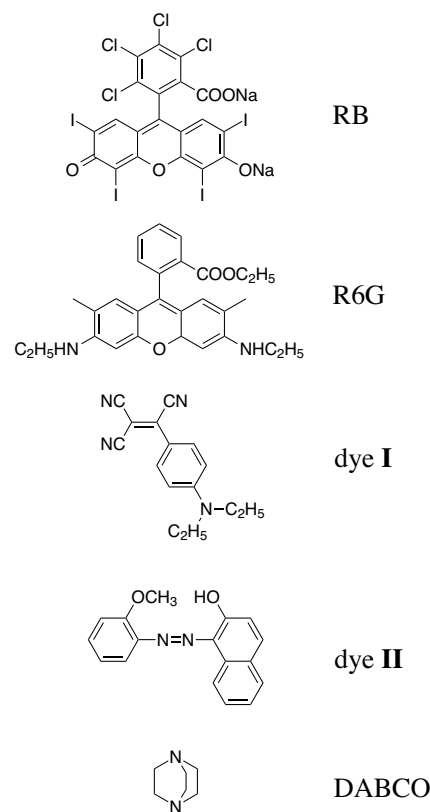


Chart 1. Structural formulae of dyes and $^1\text{O}_2$ quencher.

laser beam was imaged by an F-matched lens onto the entrance slit of a 33-cm single monochromator (Actes, CSM-330) with a grating of 600 grooves mm^{-1} . The luminescence was dispersed by the monochromator, and was detected by a liquid-nitrogen-cooled NIR photomultiplier tube (Hamamatsu, R5509-72) which had good spectral sensitivity in the wavelength region of 300 nm to 1.6 μm . The spectral slit width at 1270 nm was set to 16 nm. Wavelength calibration was done by using a mercury lamp and the Rayleigh and Raman scatterings of acetone excited by the fundamental (1064 nm) and the second harmonic (532 nm) of the Nd:YVO₄ laser. The laser beam was chopped by an optical chopper blade (Stanford Research, SR540) at approximately 2 kHz. The output of the photomultiplier tube was fed into a lock-in amplifier (NF Electronic, 5600A) with the chopper signal as a reference. The monochromator and the lock-in amplifier were controlled by a computer to record a spectrum. All the measurements were done at room temperature.

Results and Discussion

Measurement Technique of $^1\text{O}_2$ phosphorescence

Figure 1a shows the $^1\text{O}_2$ phosphorescence spectrum photosensitized by RB in aerated acetonitrile. The peak at 1272 nm is assigned to the $^1\Delta_g \rightarrow ^3\Sigma_g$ transition of O_2 . The peak height is 14 mV. The literature value of Q_Δ for RB in aerated acetonitrile is 0.54 ($\pm 20\%$),¹⁵ and we use it as the standard value in the present study.¹⁸ The replacement of RB with R6G without changing the absorbance at 532 nm resulted in a spectrum shown in Figure 1b. We can still clearly see the $^1\text{O}_2$ peak, though there are substantial background signals originated from R6G luminescence (fluorescence and phosphorescence). Stracke et al. first reported a R6G-photosensitized $^1\text{O}_2$ spectrum.¹⁰ Our present data not only reproduce theirs but also have far better quality. The spectrum in Figure 1b was fitted with a linear combination of the $^1\text{O}_2$ spectrum by RB (Figure 1a) and a parabolic base

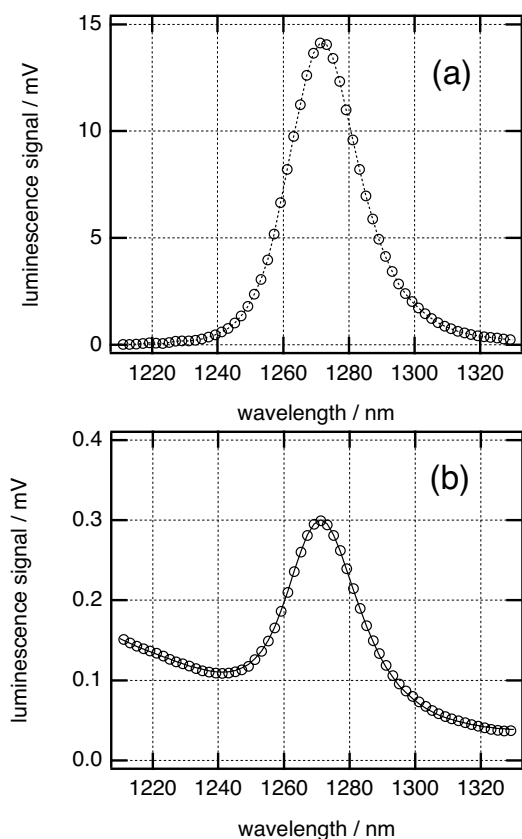


Figure 1. $^1\text{O}_2$ phosphorescence spectra photosensitized by (a) RB in aerated acetonitrile (open circles: data, dotted lines: only connecting the data points), and (b) R6G in aerated acetonitrile (open circles: data, solid curve: fitting).

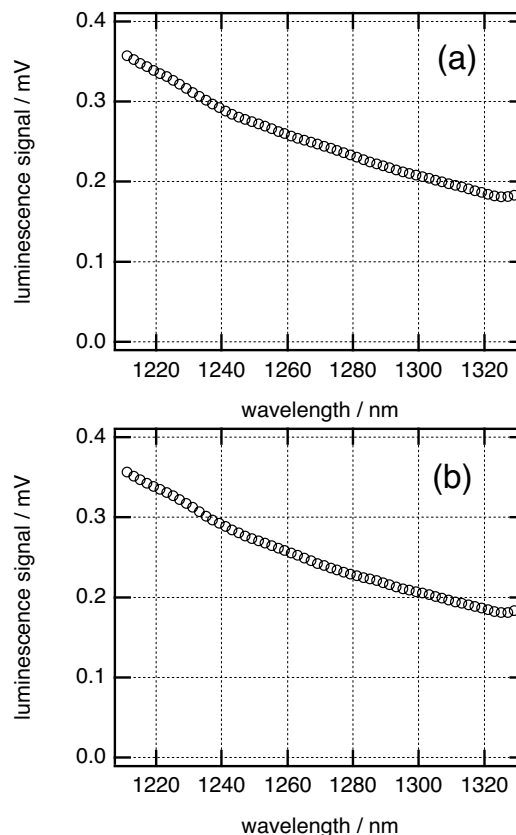


Figure 2. Luminescence spectra (long-wavelength tail) of dye I in aerated acetonitrile. (a) In the absence of DABCO. (b) In the presence of DABCO. $[\text{DABCO}] = 4.6 \times 10^{-3} \text{ mol dm}^{-3}$.

line. The fitting curve reproduces the data very well. The value of Q_Δ for R6G in aerated acetonitrile is obtained from the coefficient of the linear-combination fitting as $(8.3 \pm 1.7) \times 10^{-3}$.

In Figure 2a, we depict the luminescence spectrum obtained from dye I. There is no obvious peak at 1.27 μm . The featureless spectrum in Figure 2a is regarded as the long-wavelength tail of the dye I luminescence signals. The same measurement for dye II resulted in a similar featureless spectrum with no peak (data not shown). Though the spectrum in Figure 2a does not have the $^1\text{O}_2$ peak, we believe that there is some contribution from $^1\text{O}_2$ photosensitized by dye I buried in the luminescence background. We made another sample solution which contained dye I and DABCO. The concentration of dye I in this solution was the same as above, and that of DABCO was $4.6 \times 10^{-3} \text{ mol dm}^{-3}$. DABCO is an effective $^1\text{O}_2$ quencher,¹⁹ and we made sure that the presence of 4.6-mM DABCO reduced the phosphorescence signal of $^1\text{O}_2$ sensitized by RB in aerated

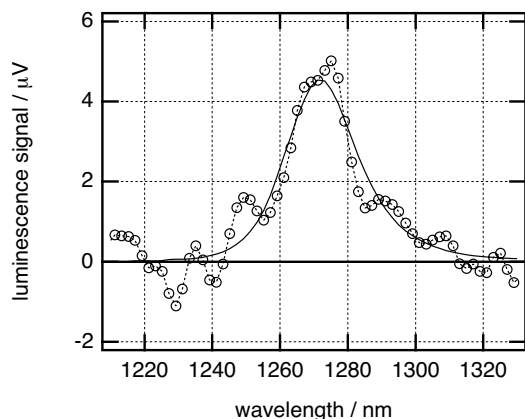


Figure 3. Difference spectrum obtained by subtracting the spectrum of dye **I** with DABCO (Figure 2b) from that of dye **I** only (Figure 2a). Open circles are data, and dotted lines only connect the data points. A solid curve indicates fitting.

acetonitrile to 0.7%. The luminescence from the solution of dye **I** with DABCO was measured in the same way, and is shown in Figure 2b. The spectrum in Figure 2b looks nearly identical with that in Figure 2a, but we think that the former is not effectively contributed to by $^1\text{O}_2$. In harmony with this thought, we can see a very small peak at $1.27 \mu\text{m}$ in a difference spectrum shown in Figure 3, which is obtained by subtracting the spectrum of dye **I** with DABCO (Figure 2b) from that of dye **I** only (Figure 2a). Note that the vertical axis of the difference spectrum is in μV . The peak is ascribed to $^1\text{O}_2$ photosensitized by dye **I**. This assignment has been confirmed by the fact that no peak was found in the difference spectra for dye **I** in nitrogen-saturated acetonitrile. The peak height in Figure 3 is $4.5 \mu\text{V}$. The difference

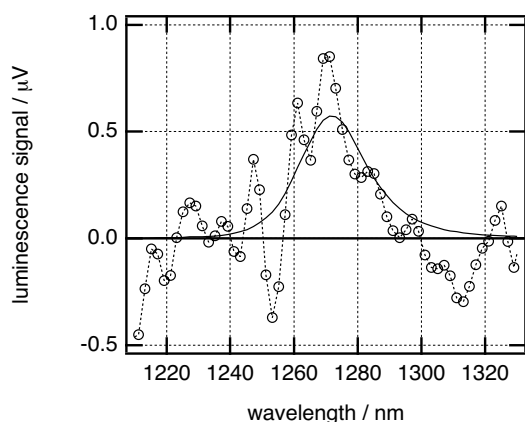


Figure 4. $^1\text{O}_2$ phosphorescence spectrum photosensitized by dye **II** in aerated acetonitrile. Open circles are data, and dotted lines only connect the data points. A solid curve indicates fitting.

spectrum is well reproduced by the $^1\text{O}_2$ spectrum from RB (Figure 1a) with a scaling factor. Q_Δ for RB multiplied by the scaling factor equals Q_Δ for dye **I**, which is calculated at $(1.7 \pm 0.5) \times 10^{-4}$. The same experimental procedure with longer accumulation time and the same data treatment for dye **II** resulted in a difference spectrum shown in Figure 4. The $^1\text{O}_2$ peak height for dye **II** is $0.6 \mu\text{V}$. The standard $^1\text{O}_2$ spectrum (Figure 1a) is multiplied by a scaling factor, and is drawn as a fitting curve in Figure 4. Q_Δ for dye **II** in aerated acetonitrile is estimated at $(2.2 \pm 1.5) \times 10^{-5}$. This value is the lowest quantum yield of $^1\text{O}_2$ formation measured and reported so far to the best of our knowledge.

Lightfastness of Dyes

We discuss relationship between Q_Δ and lightfastness in this section. The photodegradation starts from the excited states, and therefore it is important to consider the excited-state kinetics. In Figure 5, main relaxation pathways from the lowest excited singlet (S_1) state of a dye molecule are depicted. The S_1 state decays to the ground (S_0) state or the lowest excited triplet (T_1) state. The decay to the S_0 state is either radiative or nonradiative. The radiative decay corresponds to fluorescence emission. The relaxation from S_1 to T_1 is called intersystem crossing. The rates of these decay processes (k_r , k_n , k_{isc}) can be determined experimentally in the following way: the radiative decay rate (k_r) is directly calculated from the molar absorption spectrum of the dye. The quantum yield of the T_1 state ($= k_{isc} / (k_n + k_r + k_{isc})$) is in general nearly equal to or slightly higher than Q_Δ . The fluorescence quantum yield ($=$

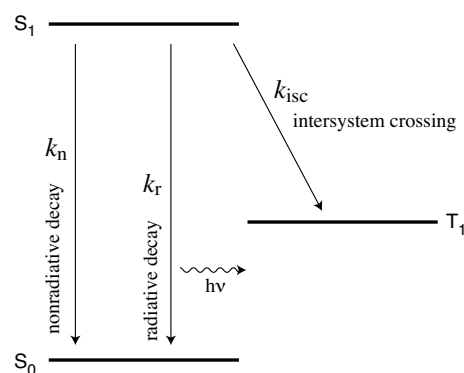


Figure 5. Schematic diagram of excited-state kinetics for dyes. k_n , k_r , and k_{isc} stand for the decay rates of each relaxation process.

Table I. Lightfastness, Q_{Δ} , and Excited-State Decay Rates of Dyes.

Dye	Lightfastness ¹⁾	Q_{Δ}	k_n^{-1} / ns	k_{isc}^{-1} / ns	k_r^{-1} / ns
R6G	89.3%	8.3×10^{-3}	5.2×10^2	6.4×10^2	5.4
I	99.7%	1.7×10^{-4}	3.4×10^{-4}	2.0	5.6
II	98.8%	2.2×10^{-5}	8.2×10^{-4}	37	8.5

1) ratio of residues after 0.3-W laser irradiation at 532 nm for 1 hour.

$k_r(k_n+k_r+k_{isc})^{-1}$) is routinely measured by using our spectrometer. Table I summarizes the decay rates, Q_{Δ} , and the lightfastness data of R6G, dyes **I** and **II**. The worst lightfastness of R6G among the three dyes is probably ascribed to its high Q_{Δ} , which is brought about by the long S_1 lifetime ($= (k_n+k_r+k_{isc})^{-1}$) of R6G. Fluorescent dyes are usually inferior in lightfastness because of the same reason. It is well-known that 1O_2 quenchers such as DABCO and nickel dibutylthiocarbamate effectively prevents the photofading of fluorescent dyes. As regards dyes **I** and **II**, on the other hand, ultrafast nonradiative relaxation makes their S_1 lifetimes very short. The very low quantum yields of fluorescence and 1O_2 formation for dyes **I** and **II** are attributed to the ultrashort S_1 lifetimes. Q_{Δ} for dye **I** is about eight times higher than that for dye **II**. It is due to the faster intersystem crossing rate of dye **II** as shown in the fifth column of Table I. Though Q_{Δ} for dye **I** is higher, Table I indicates that dye **I** is faster against light than dye **II**. It means that the lightfastness is not determined solely by Q_{Δ} . We have to take into account other photodegradation channels than singlet-oxygen mechanisms especially for dye **II**. It is also necessary to investigate, for example, the efficiency with which 1O_2 reacts chemically with the dyes. Reactivity with 1O_2 naturally depends on the molecular structure of the dyes. In fact, it is probable that the keto (hydrazone) tautomer of dye **II** is more easily photodegraded by 1O_2 attack than the enol (azo) one.^{2,6} Further studies are needed to obtain full description of the photofading processes of the three dyes.

Conclusion

We have developed the new spectroscopic method to detect 1O_2 at very low concentration. This is a

powerful tool for the study of photofading mechanisms, and provides valuable information for the development of photostable dyes. We are trying to improve the spectrometer by replacing the photomultiplier tube with a low-dark-noise one in order to increase the signal to noise ratio and lower the detection limit, and to obtain more insights into the photofading processes of dyes.

References and Notes

1. A. A. Gorman, and M. A. J. Rodgers, *J. Photochem. Photobiol. B: Biol.*, **14**, 159 (1992).
2. J. Griffiths, and C. Hawkins, *J. Chem. Soc. Perkin II*, 747 (1977).
3. P. B. Merkel, and J. W. F. Smith, *J. Phys. Chem.*, **83**, 2834 (1979).
4. K. Kotak, A. S. Schulte, J. Hay, and J. K. Sugden, *Dyes and Pigm.*, **34**, 159 (1997).
5. J. Sokolowska-Gajda, *Dyes and Pigm.*, **36**, 149 (1998).
6. L. M. G. Jansen, I. P. Wilkes, F. Wilkinson, and D. R. Worrall, *J. Photochem. Photobiol. A: Chem.*, **125**, 99 (1999).
7. F. Wilkinson, W. P. Helman, and A. B. Ross, *J. Phys. Chem. Ref. Data*, **22**, 113 (1993).
8. R. Boch, B. Mehta, T. Connolly, T. Durst, J. T. Arnason, R. W. Redmond, and J. C. Scaiano, *J. Photochem. Photobiol. A: Chem.*, **93**, 39 (1996).
9. H. Gruen, H. Steffen, and D. Schulte-Frohlinde, *J. Soc. Dye. Col.*, **97**, 430 (1981).
10. F. Stracke, M. Heupel, and E. Thiel, *J. Photochem. Photobiol. A: Chem.*, **126**, 51 (1999).
11. J. R. Hurst, J. D. McDonald, and G. B. Schuster, *J. Am. Chem. Soc.*, **104**, 2065 (1982).
12. P. R. Ogilby, and C. S. Foote, *J. Am. Chem. Soc.*, **104**, 2069 (1982).
13. R. D. Scurlock, and P. R. Ogilby, *J. Phys. Chem.*, **91**, 4599 (1987).
14. A. A. Gorman, I. Hamblett, C. Lambert, A. L. Prescott, M. A. J. Rodgers, and H. M. Spence, *J. Am. Chem. Soc.*, **109**, 3091 (1987).
15. R. Schmidt, and E. Afshari, *J. Phys. Chem.*, **94**, 4377 (1990).
16. R. Schmidt, and C. Tanielian, *J. Phys. Chem. A*, **104**, 3177 (2000).
17. A. Beeby, A. W. Parker, and C. F. Stanley, *J. Photochem. Photobiol. B: Biol.*, **37**, 267 (1997).
18. It is known that RB quenches 1O_2 sensitized by itself (Refs. 10, 17). We do not take the effect of the 1O_2 quenching into account, because Q_{Δ} correction necessitated by the quenching effect is within the uncertainty of the standard value ($0.54 \pm$

20%) and the present experimental uncertainty.

19. C. Ouannès, and T. Wilson, *J. Am. Chem. Soc.*, **90**, 6527 (1968).

Biography

Shoichi Yamaguchi earned his B.S. and M.S. degrees in Laser Physics from the University of Tokyo in 1990 and 1992 respectively. He worked as a research scien-

tist at the Kanagawa Academy of Science and Technology until 1995 when he returned to the University of Tokyo as a research assistant in Chemistry while completing his Ph.D. in Physical Chemistry (1998). Since 1998 he was a research scientist at the Yokohama Research Center of Mitsubishi Chemical Corporation. He joined the Center for Analytical Chemistry and Science, Inc. in 2000.